



CHORUS

This is the accepted manuscript made available via CHORUS. The article has been published as:

Superconductivity in the half-Heusler compound TbPdBi

H. Xiao, T. Hu, W. Liu, Y. L. Zhu, P. G. Li, G. Mu, J. Su, K. Li, and Z. Q. Mao

Phys. Rev. B **97**, 224511 — Published 13 June 2018

DOI: [10.1103/PhysRevB.97.224511](https://doi.org/10.1103/PhysRevB.97.224511)

Superconductivity in half-Heusler compound TbPdBi

H. Xiao^{1*}, W. Liu^{1,5}, Y. L. Zhu³, P. G. Li³, G. Mu^{2,4}, J. Su⁶, K. Li¹, T. Hu^{2,4§}, and Z. Q. Mao^{3#}

¹ Center for High Pressure Science and Technology Advanced Research, Beijing, 100094, China

² State Key Laboratory of Functional Materials for Informatics,

Shanghai Institute of Microsystem and Information Technology,

Chinese Academy of Sciences, 865 Changning Road, Shanghai 200050, China

³ Department of Physics and Engineering Physics,

Tulane University, New Orleans, LA 70018, USA

⁴ CAS Center for Excellence in Superconducting Electronics (CENSE), Shanghai 200050, China

⁵ Department of Physics, Zhejiang SCI-TECH University, Hangzhou, 310018, China and

⁶ College of Chemistry and Molecular Engineering, Peking University, Beijing 100871, China

(Dated: May 29, 2018)

We have studied the half-Heusler compound TbPdBi through resistivity, magnetization, Hall effect and heat capacity measurements. A semimetal behavior is observed in its normal state transport properties, which is characterized by a large negative magnetoresistance below 100 K. Notably, we find the coexistence of superconductivity and antiferromagnetism in this compound. The superconducting transition appears at 1.7 K, while the antiferromagnetic phase transition takes place at 5.5 K. The upper critical field H_{c2} shows an unusual linear temperature dependence, implying unconventional superconductivity. Moreover, when the superconductivity is suppressed by magnetic field, its resistivity shows plateau behavior, a signature often seen in topological insulators/semimetals. These findings establish TbPdBi as a new platform for study of the interplay between superconductivity, magnetism and non-trivial band topology.

A. Introduction

The large family of ternary half-Heusler compounds with non-centrosymmetric structure, formulated as XYZ (X = rare earth elements, Y = transition-metal elements, Z = main-group elements), has recently attracted a great deal of interests.¹⁻⁴ In particular, the $RPdBi$ and $RPtBi$ (R = rare earth) half Heusler series have shown to be an interesting platform for the study of unconventional superconductivity. For instance, $YPtBi$ and $LuPtBi$ have been reported to be superconducting,⁵⁻¹³ (their T_c values are 0.77 K and 1 K respectively) even though they have a surprisingly low carrier concentration, i.e. $n = 10^{18}$ - 10^{19} cm^{-3} .^{5,6,10} There have been compelling evidences which show the superconductivity in these compounds are unconventional. The low-temperature penetration depth measurements on $YPtBi$ has revealed that its superconducting gap has nodes.¹⁴ In addition, the unusual linear temperature dependence of the upper critical field points to an odd parity component in the superconducting order parameter, in accordance with the predictions for non-centrosymmetric superconductors.⁶ Due to strong spin-orbital coupling, the superconducting state of $YPtBi$ is believed to have a mixture of a conventional pairing state and high-angular momentum pairing states.¹⁵⁻²⁰ For $LuPtBi$, a surface nodal superconducting state has been observed with its T_c being much higher than that in the bulk.²¹

In this paper, we report resistivity, magnetization, Hall effect and heat capacity measurements on the half Heusler compound TbPdBi. For the first time, we observed superconductivity in this compound with an onset temperature of $T_c = 1.7$ K, besides the antiferromagnetic transition at $T_N = 5.5$ K. Unlike other half-Heusler su-

perconductors which feature semi-metallic normal states with large positive magnetoresistance, the superconductivity of TbPdBi is connected with an unusual normal state characterized by a large isotropic negative magnetoresistance. Regardless of this difference, TbPdBi exhibits a linear temperature dependence in upper critical field H_{c2} , similar to other half-Heusler superconductors, suggesting TbPdBi also possesses unconventional superconductivity. When its superconductivity is suppressed by magnetic field, its resistivity as a function of temperature shows a plateau behavior, suggesting the possible presence of non-trivial band topology. These results establish TbPdBi as an intriguing platform for the study of the interplay between unconventional superconductivity, magnetism and non-trivial band topology.

B. Experimental Details

Single crystals of TbPdBi were grown using Bi flux. We have performed single-crystal X-ray diffraction (XRD) measurements on TbPdBi. The data were collected at 293(2)K on a Rigaku XtaLAB PRO 007HF(Mo) diffractometer, with Mo $K\alpha$ radiation ($\lambda = 0.71073$ Å). Data reduction and empirical absorption correction were performed using the CrysAlisPro program. The structure was solved by a dual-space algorithm using SHELXT program. Final structure refinement was done using the SHELXL program by minimizing the sum of squared deviations of F^2 using a full-matrix technique. Table 1 summarizes the detailed structural parameters extracted from the structural refinement, which shows the sample used in our study indeed has a cubic $F\bar{4}3m$ crystal structure. The occupancy of each element obtained from the refinement is close to 1, suggesting the composition of our

TABLE I. Structural parameters of TbPdBi determined by single crystal XRD measurements at 293(2) K. Space group: $F\bar{4}3m$ (No. 216). Lattice parameters: $a = 6.65310(10)$ Å, $b = 6.65310(10)$ Å, $c = 6.65310(10)$ Å, $\alpha = \beta = \gamma = 90^\circ$. $R_1 = 0.0351$; $wR_2 = 0.0836$; U_{eq} is defined as one-third of the trace of the orthogonalized U_{ij} tensor (Å²).

Atom	Wyckoff.	Occupancy.	x	y	z	U_{eq}
Bi	4b	1	1/2	1/2	1/2	0.0089(11)
Tb	4a	1	0	0	0	0.0112(16)
Pd	4d	1	3/4	3/4	3/4	0.013(2)

78 synthesized compound is close to be stoichiometric, i.e.
 79 TbPdBi. For transport measurements, the sample was
 80 first sanded and then cut into small pieces. The thick-
 81 ness of the sample used is about 35 μm . The resistivity is
 82 measured down to 50 mK by using a dilution refrigerator
 83 in a physical properties measurement system (PPMS).
 84 DC susceptibility was measured down to 2 K. Heat ca-
 85 pacity were measured by a relaxation time method.

86 C. Results and Discussion

87 Figure 1(a) shows the temperature T dependent resistivity ρ measured under different applied magnetic fields
 88 ($H = 0, 1, 3, 5, 9$ T). As cooling down from room temper-
 89 ature, the resistivity demonstrates a semiconductor-like
 90 behavior above certain temperature T_{peak} . Below that,
 91 it shows a metallic behavior. This behavior is charac-
 92 teristic of semimetals or narrow-gap semiconductors as
 93 observed previously in half-Heusler compound.^{22,23} The
 94 position of T_{peak} , marked by a downward arrow, shifts to
 95 higher temperature with increasing magnetic field, which
 96 is summarized in inset to Fig. 1(a). At higher temper-
 97 atures ($T > 100$ K), the resistivity curves measured in
 98 different H merge into one single curve, while large neg-
 99 ative magnetoresistivity (MR) is observed at low temper-
 100 atures ($T < 100$ K). This can be seen more clearly from
 101 Fig. 1(b) and its inset, which plots the T dependence of
 102 $\rho(9\text{T})/\rho(0\text{T})-1$ and the H dependence of $\rho(H)/\rho(0\text{T})-1$,
 103 respectively.

104 The large negative MR (up to 80%) is a remarkable
 105 signature, contrasted with the nearly zero MR above
 106 T_{peak} . However, it is not clear yet about the origin of
 107 the negative MR and further study is needed to under-
 108 stand it. Note that for ordinary non-magnetic metal,
 109 the MR is usually weak and positive. In half-Heusler
 110 compounds, the MR is found to be positive and large.
 111 For example, in LuPtBi, positive MR as large as 3200%
 112 is reported.¹¹ Negative and high anisotropic MR is re-
 113 ported in Weyl semimetals, such as TaAs-class materials,
 114 and has been regarded as the most prominent transport
 115 signature caused by the chiral anomaly effect.²⁴ However,
 116 our observation of the negative MR in TbPdBi is nearly
 117 independent of field orientation. Thus the negative MR
 118 observed in present case can not be understood in terms

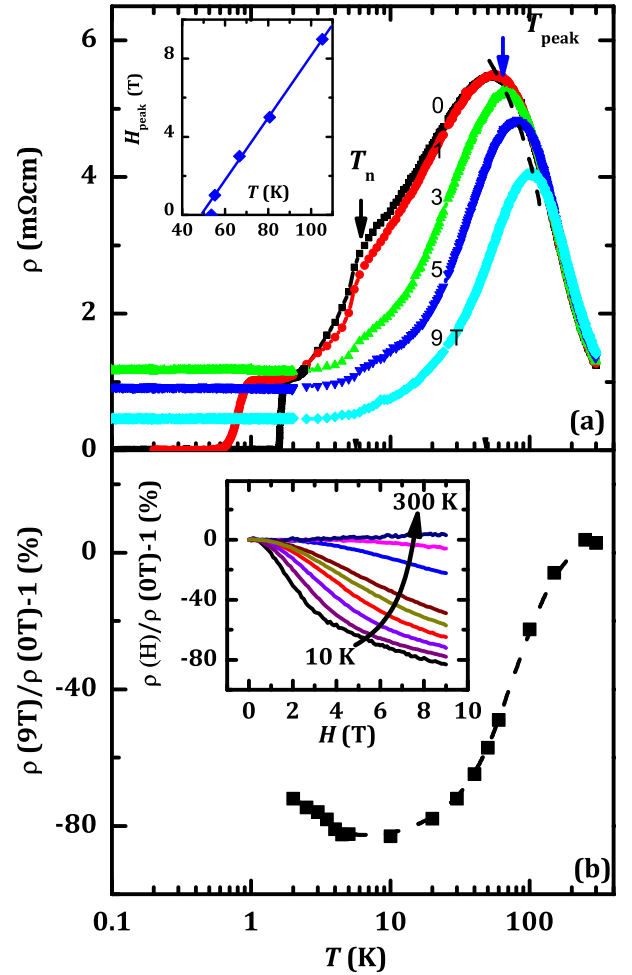


FIG. 1. (a) The resistivity ρ vs. temperature T data for TbPdBi from 50 mK to 300 K under applied magnetic field $H = 0, 1, 3, 5, 9$ T. Inset: the T dependence of the resistivity peak in different magnetic field, H_{peak} . (b) The magnetoresistivity $\rho(9\text{T})/\rho(0\text{T})-1$ vs. temperature T . Inset shows $\rho(H)/\rho(0\text{T})-1$ vs. H at different temperatures, $T = 2, 10, 20, 30, 40, 50, 60, 100, 150, 300$ K.

120 of any existing model.

121 Below T_{peak} , the resistivity curve shows a kink at 5.5
 122 K, which can be seen more clearly from the enlarged part
 123 of the low temperature resistivity curve (Fig. 2(a), left
 124 axis). Such a resistivity kink is due to an antiferromag-
 125 netic (AFM) phase transition previously determined by
 126 neutron diffraction measurements.²³ The magnetization
 127 M vs. T curves measured at $H = 1$ kOe in both zero
 128 field cooled (ZFC) and field cooled (FC) conditions are
 129 also shown in Fig. 2(a) (right axis), which suggest an
 130 AFM transition at $T_N = 5.5$ K. Below T_N , the magne-
 131 tization shows irreversibility, which may be caused by
 132 moment canting. Note that below T_N , the magnitude of
 133 the magnetoresistivity $\rho(9\text{T})/\rho(0\text{T})-1$ decreases with de-
 134 creasing temperature, although it remains negative (see
 135 Fig. 1(b)).

136 With further decreasing temperature, the resistivity

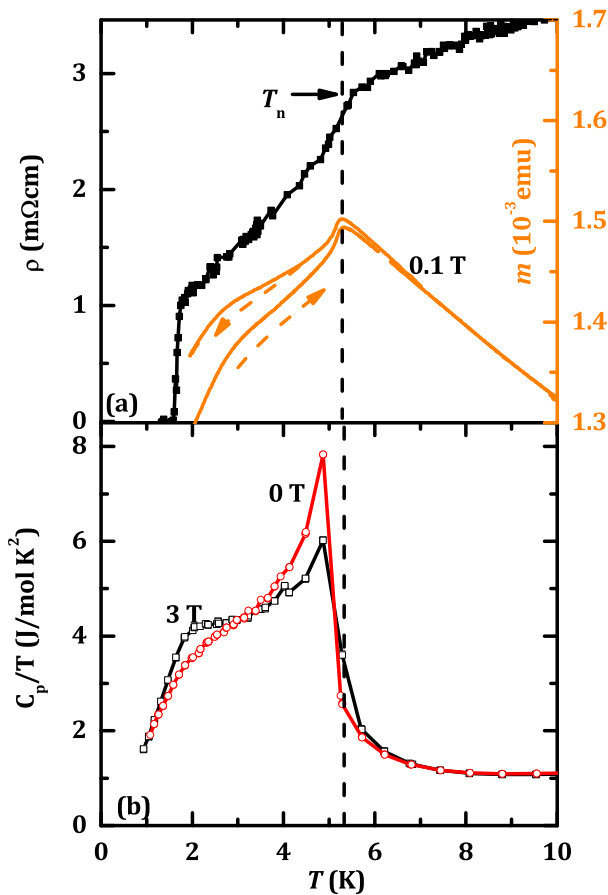


FIG. 2. (a) Left axis: The low temperature part of the ρ vs. T curve at zero magnetic field. Right axis: Magnetization measurements on TbPdBi with applied magnetic field $H = 1$ kOe in zero field cool (ZFC) and field cool (FC) conditions. (b) The temperature T dependence of the specific heat ratio C_p/T at $H = 0$ and $H = 3$ T.

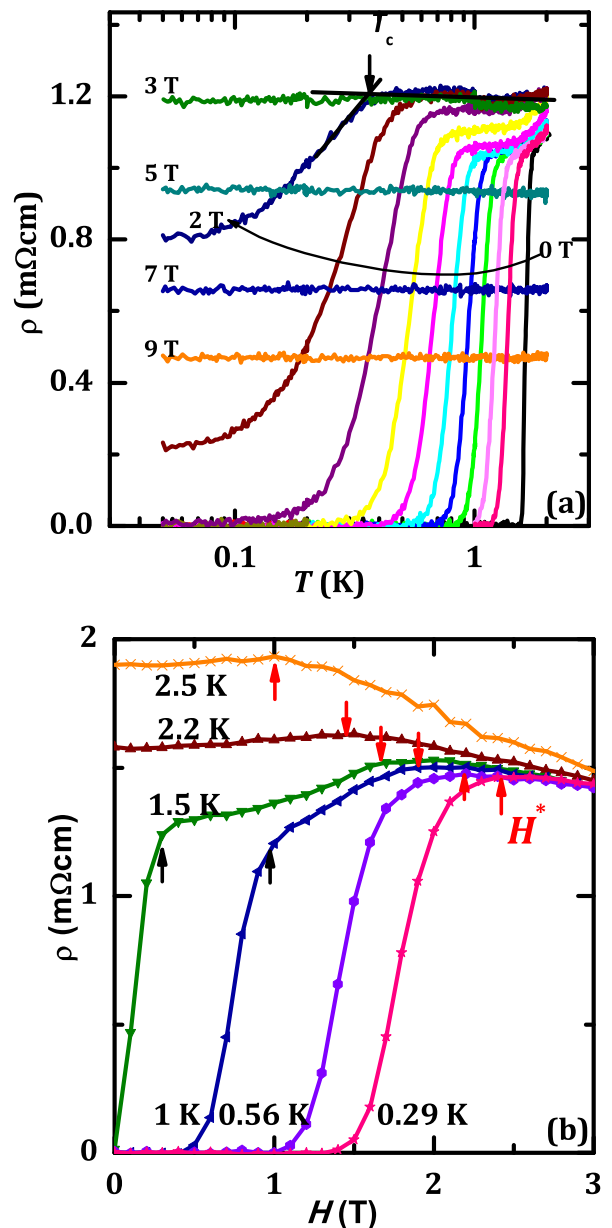


FIG. 3. (a) The resistivity ρ vs. temperature T for TbPdBi measured in a dilution refrigerator with applied magnetic field $H = 0, 0.2, 0.4, 0.6, 0.8, 1, 1.2, 1.4, 1.6, 1.8, 2, 3, 5, 7,$ and 9 T. (b) The resistivity ρ vs. magnetic field H for TbPdBi at different temperatures, $T = 0.29, 0.56, 1, 1.5, 2.2,$ and 2.5 K.

137 drops sharply at 1.7 K, down to zero at 1.58 K, sig-
 138 naling an onset superconducting transition at 1.7 K.
 139 The T_c of 1.7 K is almost the same as that of LuPdBi
 140 which was reported to have the highest superconduct-
 141 ing transition temperature among the superconductors
 142 found in the half Heusler family or other noncentrosym-
 143 metric systems.²⁵ Although TbPdBi was previously stud-
 144 ied, its superconductivity was not reported.²³ Previous
 145 transport measurements showed its resistivity exhibits
 146 a tendency of drop at about 0.5 K, but does not de-
 147 creases to zero.²³ This implies the sample used in our
 148 study somewhat differs from the sample used in previ-
 149 ous work. In order to clarify such a possible sample de-
 150 pendence of superconductivity, we have examined sev-
 151 eral samples from different batches and found all of them
 152 show superconductivity. We also compared the transport
 153 measurements on the samples whose leads are prepared
 154 using silver paste and silver epoxy respectively. The sil-
 155 ver paste did not require baking, while the silver epoxy
 156 did. Both samples also showed the same superconductiv-

157 ity, which excludes the possibility that the superconduct-
 158 ing phase we observed in TbPdBi is induced by heating.
 159 One possible reason for the difference between our sample
 160 and the reported one²³ is that the reported sample likely
 161 involves non-stoichiometry, causing inhomogeneous su-
 162 perconductivity. The tendency of resistivity drop below
 163 0.5 K observed in the reported sample is indeed a sig-
 164 nature of inhomogeneous superconductivity. Note that
 165 recent penetration depth measurements also verified the
 166 superconductivity of TbPdBi.²⁶

We also performed specific heat measurements on the TbPdBi sample. Figure 2(b) shows the temperature dependence of the specific heat ratio, C_P/T , measured at $H = 0$ and $H = 3$ T. From the zero field specific heat data, it is found that there is a sharp jump at $T_N = 4.86$ K, which is coincident with the antiferromagnetic phase transition probed by resistivity and magnetization measurements. The magnitude of the jump is in the order of $J/\text{mol K}^2$, consistent with the previous report,²³ suggesting a huge release of magnetic entropy. With $H = 3$ T, the peak position of C_P/T remains unchanged but the magnitude of the peak gets suppressed. In addition, the 0 T data shows a humplike anomaly at lower temperatures, which is likely to originate from the change of spin structure. However, we did not observe a clear superconducting anomaly in C/T at T_c , similar to the scenario seen in other half Heusler superconductors such as YPtBi⁹ and HoPtBi.²⁷ This can possibly be attributed to small effective mass of quasi-particles, thus resulting in electronic specific anomaly being too small to be observed.

Figure 3(a) shows the ρ vs. T curves measured under different applied magnetic field $H = 0, 0.2, 0.4, 0.6, 0.8, 1, 1.2, 1.4, 1.6, 1.8, 2, 3, 5, 7,$ and 9 T below 2 K. With increasing magnetic fields, the superconducting transition temperature is gradually suppressed to zero and the transition width becomes broader. The onset of the superconducting transition temperature T_c^{onset} is defined as the cross point of the two extrapolated straight lines, as shown in Fig. 3(a). In zero magnetic field, T_c^{onset} is determined to be 1.7 K. Based on these data, we obtain the temperature dependence of the upper critical field H_{c2} , as shown in Fig. 4(a) (circles). Note that H_{c2} shows almost linear behavior in the whole measured temperature range and there is no sign of saturation at low temperatures, similar to what is observed in YPtBi.⁵

The value of H_{c2} at 0 K estimated from linear extrapolation is 2.4 T. Here we can estimate the superconducting coherence length at zero temperature, $\xi = (\frac{\Phi_0}{2\pi H_{c2}})^{1/2} = 12$ nm. Note that the value of H_{c2} for TbPdBi is comparable with that of other RPdBi/RPtBi superconductors. For example, $H_{c2}(0)$ is 2.2 T for LuPdBi²⁵ and 1.5 T for YPtBi.⁵ We also evaluate the orbital limiting field using the weak-coupling Werthamer-Helfand-Hohenberg (WHH) formula in the clean limit, $H_{orb} = 0.69T_c[-dH_{c2}/dT]_{T_c} = 1.8$ T. The Pauli limiting field $H_p = \Delta/(\sqrt{2}\mu_B)$ where $\Delta = 1.76k_B T_c$ can be estimated to be 3.2 T. Since $H_{orb} < H_{c2} < H_p$, superconductivity in TbPdBi is orbital limited. But the fact that H_{c2} is larger than the weak-coupling WHH estimation of H_{orb} indicates that spin-orbital coupling is important in this material. In addition, the linear temperature dependence of H_{c2} suggests an unusual superconducting state. In the absence of inversion center, this may point to a possible mixed singlet-triplet pairing state.¹⁰

It is interesting to note that a resistivity plateau emerges at low temperatures when the superconductivity is completely suppressed above $H = 3$ T (see Fig.

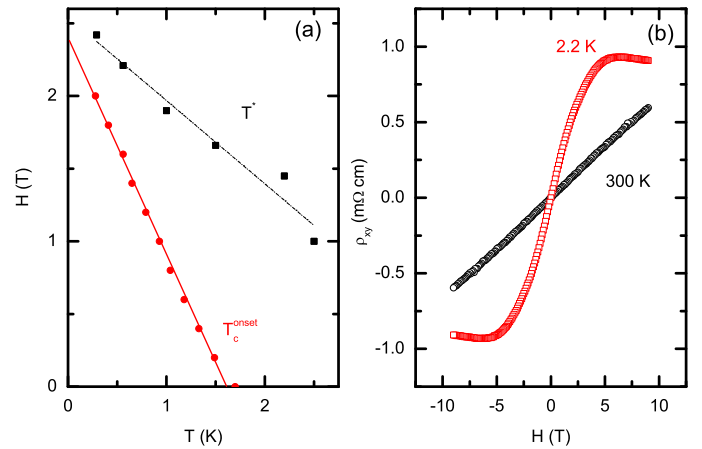


FIG. 4. (a) The magnetic field H vs. temperature T phase diagram. The circles represent the onset superconducting transition temperature T_c^{onset} . The squares denotes T^* , the crossover temperature of the positive MR to negative MR behavior at low temperatures. (b) The hall resistivity ρ_{xy} vs. magnetic field H at $T = 2.2$ and 300 K.

3(a)). For a topological insulator (TI), the surface which is in contact with air is metallic whereas the bulk is insulating, as a result of time reversal symmetry protecting the metallic surface modes of topological insulators. The transport signature of such a surface state is a plateau that arrests the exponential divergence of the insulating bulk with decreasing temperature. A resistivity plateau is reported in $\text{Bi}_2\text{Te}_2\text{Se}$,²⁸ SmB_6 ,²⁹ LaSb ,³⁰ TaSb_2 ,³¹ and also in similar half Heusler compound LuPtBi.¹¹ Hence, the resistivity plateau observed in TbPdBi implies that its electronic band structure involves non-trivial band topology. Further band structure calculations and ARPES measurements are needed to reveal its nature.

Fig. 3(b) shows the H dependence of the ρ at several selected temperatures, $T = 0.29, 0.56, 1, 1.5, 2.2$ and 2.5 K. Note that there is a crossover from positive MR to negative MR behavior at $H^*(T^*)$, which disappears at higher temperatures. Fig. 4(a) (squares) shows the magnetic field dependence of T^* , which increases with decreasing magnetic field. The origin of $H^*(T^*)$ (position of MR peak) and its relationship to the superconductivity is not clear yet which requires further study.

The Hall resistivity ρ_{xy} vs magnetic field H at $T = 2.2$ and 300 K is plotted in Fig. 4(b). At $T = 300$ K, the linear dependence of ρ_{xy} on the magnetic field indicate that one type of charge carrier dominates the transport properties at this particular temperature. Based on the one-carrier model, the carrier density n is then estimated to be $9.43 \times 10^{18} \text{cm}^{-3}$, comparable with other half-Heusler compounds.^{5,23,25} Such a low carrier density might explain why the specific heat data do not exhibit a discernible signature of T_c . At low temperatures, $T = 2.2$ K, ρ_{xy} is no longer linearly dependent on H , suggesting more complicated band structure. This is different from LuPdBi, where ρ_{xy} is linear in H at both $T = 2$ K and

260 $T = 300$ K.²⁵

271 states, superconductivity and magnetism.

261 D. Summary

262 In summary, we report superconductivity with T_c of 1.7
 263 K in antiferromagnetic half-Heusler compound TbPdBi,
 264 which has an unusual normal state with large nega-
 265 tive magnetoresistivity. The resistivity plateau at low
 266 temperature under magnetic field suggests possible non-
 267 trivial band topology. The upper critical field H_{c2} shows
 268 unusual linear dependence on temperature, implying un-
 269 conventional superconductivity. Thus, TbPdBi provides
 270 a new platform to study the interplay of topological

272 E. Acknowledgments

273 We thanks Peijie Sun from IOP, CAS, Haiyan Zheng,
 274 Xiaohuan Lin from HPSTAR, and Hui Zhang from
 275 SIMIT for helpful discussions. Work at HPSTAR was
 276 supported by NSAF, Grant No. U1530402. Work at
 277 SIMIT was supported by NSFC, Grant No. 11574338.
 278 The efforts of sample growth and a part of data analysis
 279 at Tulane were supported by the U. S. Department of
 280 Energy under EPSCOR Grant No. DE-SC0012432 with
 281 additional support from Louisiana Board of Regents.
 282 * hong.xiao@hpstar.ac.cn § thu@mail.sim.ac.cn #
 283 zmao@tulane.edu

-
- 284 ¹ W. Al-Sawai, H. Lin, R. S. Markiewicz, L. A. Wray, Y. Xia,
 285 S.-Y. Xu, M. Z. Hasan, and A. Bansil, *Phys. Rev. B* **82**,
 286 125208 (2010).
 287 ² D. Xiao, Y. Yao, W. Feng, J. Wen, W. Zhu, X.-Q. Chen,
 288 G. M. Stocks, and Z. Zhang, *Phys. Rev. Lett.* **105**, 096404
 289 (2010).
 290 ³ S. Chadov, X. Qi, J. Kbler, G. H. Fecher, C. Felser, and
 291 S. C. Zhang, *Nature Materials* **9**, 541 (2010).
 292 ⁴ H. Lin, L. A. Wray, Y. Xia, S. Xu, S. Jia, R. J. Cava,
 293 A. Bansil, and M. Z. Hasan, *Nat Mater* **9**, 546 (2010).
 294 ⁵ N. P. Butch, P. Syers, K. Kirshenbaum, A. P. Hope, and
 295 J. Paglione, *Phys. Rev. B* **84**, 220504 (2011).
 296 ⁶ T. V. Bay, T. Naka, Y. K. Huang, and A. de Visser, *Phys.*
 297 *Rev. B* **86**, 064515 (2012).
 298 ⁷ M. Meinert, *Phys. Rev. Lett.* **116**, 137001 (2016).
 299 ⁸ A. Kronenberg, J. Braun, J. Minár, H.-J. Elmers, D. Kut-
 300 nyakhov, A. V. Zaporozhchenko, R. Wallauer, S. Chern-
 301 nov, K. Medjanik, G. Schönhense, M. Kläui, S. Chadov,
 302 H. Ebert, and M. Jourdan, *Phys. Rev. B* **94**, 161108
 303 (2016).
 304 ⁹ O. Pavlosiuk, D. Kaczorowski, and P. Wiñiewski, *Phys.*
 305 *Rev. B* **94**, 035130 (2016).
 306 ¹⁰ F. F. Tafti, T. Fujii, A. Juneau-Fecteau, S. René de Cotret,
 307 N. Doiron-Leyraud, A. Asamitsu, and L. Taillefer, *Phys.*
 308 *Rev. B* **87**, 184504 (2013).
 309 ¹¹ Z. Hou, W. Wang, G. Xu, X. Zhang, Z. Wei, S. Shen,
 310 E. Liu, Y. Yao, Y. Chai, Y. Sun, X. Xi, W. Wang, Z. Liu,
 311 G. Wu, and X.-x. Zhang, *Phys. Rev. B* **92**, 235134 (2015).
 312 ¹² C. Liu, Y. Lee, T. Kondo, E. D. Mun, M. Caudle, B. N.
 313 Harmon, S. L. Bud'ko, P. C. Canfield, and A. Kaminski,
 314 *Phys. Rev. B* **83**, 205133 (2011).
 315 ¹³ E. Mun, S. L. Bud'ko, and P. C. Canfield, *Phys. Rev. B*
 316 **93**, 115134 (2016).
 317 ¹⁴ Y. N. R. H. S. Z.-P. S. L. W. H. H. J. D. D. P. M. R. B.
 318 D. F. A. M. A. T. R. P. Hyunsoo Kim, Kefeng Wang and
 319 J. Paglione, *arXiv:1603.03375v1* (2016), 1.
 320 ¹⁵ P. M. R. Brydon, L. Wang, M. Weinert, and D. F. Agter-
 321 berg, *Phys. Rev. Lett.* **116**, 177001 (2016).
 322 ¹⁶ W. Yang, T. Xiang, and C. Wu, *Phys. Rev. B* **96**, 144514
 323 (2017).
 324 ¹⁷ L. Savary, J. Ruhman, J. W. F. Venderbos, L. Fu, and
 325 P. A. Lee, *Phys. Rev. B* **96**, 214514 (2017).
 326 ¹⁸ J. W. F. Venderbos, L. Savary, J. Ruhman, P. A. Lee, and
 327 L. Fu, *Phys. Rev. X* **8**, 011029 (2018).
 328 ¹⁹ I. Boettcher and I. F. Herbut, *Phys. Rev. Lett.* **120**, 057002
 329 (2018).
 330 ²⁰ B. Roy, M. P. Kennett, K. Yang, and V. Juricic, (2018),
 331 *arXiv:1802.02134 [cond-mat.mes-hall]*.
 332 ²¹ C. A. P. W. E. L.-F. A. K. S. C. B. Y. A. Banerjee, A. Fang
 333 and C. Felser, *March Meeting 2015 abstract T25.00005*
 334 (2015), 1.
 335 ²² K. Gofryk, D. Kaczorowski, T. Plackowski, A. Leithe-
 336 Jasper, and Y. Grin, *Phys. Rev. B* **84**, 035208 (2011).
 337 ²³ Y. Nakajima, R. Hu, K. Kirshenbaum, A. Hughes,
 338 P. Syers, X. Wang, K. Wang, R. Wang, S. R.
 339 Saha, D. Pratt, J. W. Lynn, and J. Paglione, *Science Advances* **1**
 340 (2015), 10.1126/sciadv.1500242,
 341 <http://advances.sciencemag.org/content/1/5/e1500242.full.pdf>.
 342 ²⁴ X. Huang, L. Zhao, Y. Long, P. Wang, D. Chen, Z. Yang,
 343 H. Liang, M. Xue, H. Weng, Z. Fang, X. Dai, and G. Chen,
 344 *Phys. Rev. X* **5**, 031023 (2015).
 345 ²⁵ G. Xu, W. Wang, X. Zhang, Y. Du, E. Liu, S. Wang,
 346 G. Wu, Z. Liu, and X. X. Zhang, *Scientific Reports* **4**,
 347 5709 (2014).
 348 ²⁶ S. M. A. Radmanesh, Y. L. Zhu, Z. Q. Mao, and L. Spinu,
 349 to be submitted (2018).
 350 ²⁷ O. Pavlosiuk, D. Kaczorowski, X. Fabreges, A. Gukasov,
 351 and P. Wiñiewski, *Scientific Reports* **6**, 18797 (2016).
 352 ²⁸ Z. Ren, A. A. Taskin, S. Sasaki, K. Segawa, and Y. Ando,
 353 *Phys. Rev. B* **82**, 241306 (2010).
 354 ²⁹ D. J. Kim, S. Thomas, T. Grant, J. Botimer, Z. Fisk, and
 355 J. Xia, *Scientific Reports* **3**, 3150 (2013).
 356 ³⁰ F. F. Tafti, Q. D. Gibson, S. K. Kushwaha, N. Hal-
 357 dolaarachchige, and R. J. Cava, *Nat Phys* **12**, 272 (2016).
 358 ³¹ Y. Li, L. Li, J. Wang, T. Wang, X. Xu, C. Xi, C. Cao, and
 359 J. Dai, *Phys. Rev. B* **94**, 121115 (2016).